Cell Cycle–Dependent and Schedule-Dependent Antitumor Effects of Sorafenib Combined with Radiation

John P. Plastaras,[1,2] Seok-Hyun Kim,[1] Yingqiu Y. Liu,[1] David T. Dicker,[1] Jay F. Dorsey,[1,2] James McDonough,[2] George Cerniglia,[2] Ramji R. Rajendran,[2] Anjali Gupta,[2] Anil K. Rustgi,[3] J. Alan Diehl,[4] Charles D. Smith,[6] Keith T. Flaherty,[5] and Wafik S. El-Deiry[1]

[1]Laboratory of Molecular Oncology and Cell Cycle Regulation, Departments of Medicine (Hematology/Oncology), Genetics, and Pharmacology, Institute for Translational Medicine and Therapeutics, and Abramson Cancer Center, [2]Department of Radiation Oncology, [3]Department of Medicine (Gastroenterology) and Genetics, and Abramson Cancer Center, [4]Department of Cancer Biology, and Abramson Cancer Center, and [5]Department of Medicine (Hematology/Oncology), and Abramson Cancer Center, University of Pennsylvania School of Medicine, Philadelphia, Pennsylvania and [6]Department of Pharmacology, Pennsylvania State University, Hershey, Pennsylvania

Abstract

The antineoplastic drug sorafenib (BAY 43-9006) is a multikinase inhibitor that targets the serine-threonine kinase B-Raf as well as several tyrosine kinases. Given the numerous molecular targets of sorafenib, there are several potential anticancer mechanisms of action, including induction of apoptosis, cytostasis, and antiangiogenesis. We observed that sorafenib has broad activity in viability assays in several human tumor cell lines but selectively induces apoptosis in only some lines. Sorafenib was found to decrease Mcl-1 levels in most cell lines tested, but this decrease did not correlate with apoptotic sensitivity. Sorafenib slows cell cycle progression and prevents irradiated cells from reaching and accumulating at G_2-M. In synchronized cells, sorafenib causes a reversible G_1 delay, which is associated with decreased levels of cyclin D1, Rb, and phosphorylation of Rb. Although sorafenib does not affect intrinsic radiosensitivity using *in vitro* colony formation assays, it significantly reduces colony size. In HCT116 xenograft tumor growth delay experiments in mice, sorafenib alters radiation response in a schedule-dependent manner. Radiation treatment followed sequentially by sorafenib was found to be associated with the greatest tumor growth delay. This study establishes a foundation for clinical testing of sequential fractionated radiation followed by sorafenib in gastrointestinal and other malignancies. [Cancer Res 2007;67(19):9443–54]

Introduction

Sorafenib was developed as a Raf kinase inhibitor that could therapeutically target the mutated B-Raf oncogene in malignant melanoma. Although sorafenib was not efficacious as a single agent in melanoma therapy (1), early clinical trial data suggested promising results in combination chemotherapy in melanoma (2, 3). Surprisingly, sorafenib showed efficacy in renal cell cancer and was approved in 2005 by the Food and Drug Administration as standard therapy. The activity of sorafenib in renal cell cancer seems related to an antiangiogenic effect likely due to its inhibitory effect toward vascular endothelial growth factor receptors (VEGFR) and their targets. In fact, sorafenib seems to target multiple kinases, including c-Raf, wild-type and V599E mutant B-Raf, VEGFR2, VEGFR3, Flt3, platelet-derived growth factor receptor-β, c-KIT, fibroblast growth factor receptor 1, p38α, and RET. The broad spectrum of kinase inhibitory activity of sorafenib supports the idea that it may have activity in multiple tumor types possibly when combined with other treatments.

To investigate the activity of sorafenib in gastrointestinal and other tumors, we explored its effects on cell growth of multiple human tumor cell lines. We observed a cell cycle inhibitory effect in all human tumor cell lines tested as well as apoptosis in a subset of lines. Detailed cell cycle analysis revealed that sorafenib causes a delay in the G_1 phase. Mechanistic studies revealed effects of sorafenib on cyclin D1 and Rb expression. Because of the effect of sorafenib in delaying early-phase cell cycle progression, we hypothesized that either sorafenib pretreatment followed by radiation or concurrent treatment may reduce the antitumor effects of radiation therapy. We tested this hypothesis in animal models using bioluminescence imaging and various schedules of administration of sorafenib and radiation. Although concurrent administration of sorafenib and radiation was not clearly inferior in terms of *in vivo* antitumor effect, sequential treatment using fractionated radiotherapy followed by sorafenib seemed to be the optimal schedule for combined administration of these agents. These studies lay the groundwork for clinical trials testing the safety and efficacy of sorafenib combined with ionizing radiation in gastrointestinal and other malignancies.

Materials and Methods

Reagents. Sorafenib was synthesized as described previously (4). For cell culture experiments, it was dissolved in DMSO to make a 32 mmol/L stock solution and stored at 4°C. For mouse experiments, sorafenib was dissolved in 1:1 cremophor EL (Sigma)/ethanol to make a 24 mg/mL solution. This solution was freshly diluted each day to 6 mg/mL in sterile water. A stock solution of 5 mg/mL 3-(4,5-dimethylthiazol-2-yl)-2,5-diphenyltetrazolium bromide (MTT) in PBS was stored at −20°C. Solutions of 4 mg/mL aphidicolin (Sigma) in DMSO were stored at −20°C.

Cell lines and tissue culture. $Bax^{-/-}$ HCT116 cells were provided by Bert Vogelstein (Johns Hopkins University, Baltimore, MD; ref. 5) and cultured in McCoy's 5A medium. Other cell lines were obtained from the American Type Culture Collection and cultured in the following media: RPMI 1640 (H460 and SK-Br-3) McCoy's 5A (HCT116, SKOV3, and U2OS),

Note: Supplementary data for this article are available at Cancer Research Online (http://cancerres.aacrjournals.org/).

Current address for C.D. Smith: Medical University of South Carolina, Charleston, South Carolina.

Presented at the 96th Annual Meeting of the AACR, April 2006, Washington, District of Columbia.

Requests for reprints: Wafik S. El-Deiry, University of Pennsylvania School of Medicine, 415 Curie Boulevard, CRB 437A, Philadelphia, PA 19104. Phone: 215-898-9015; Fax: 215-573-9139; E-mail: wafik@mail.med.upenn.edu.

doi:10.1158/0008-5472.CAN-07-1473

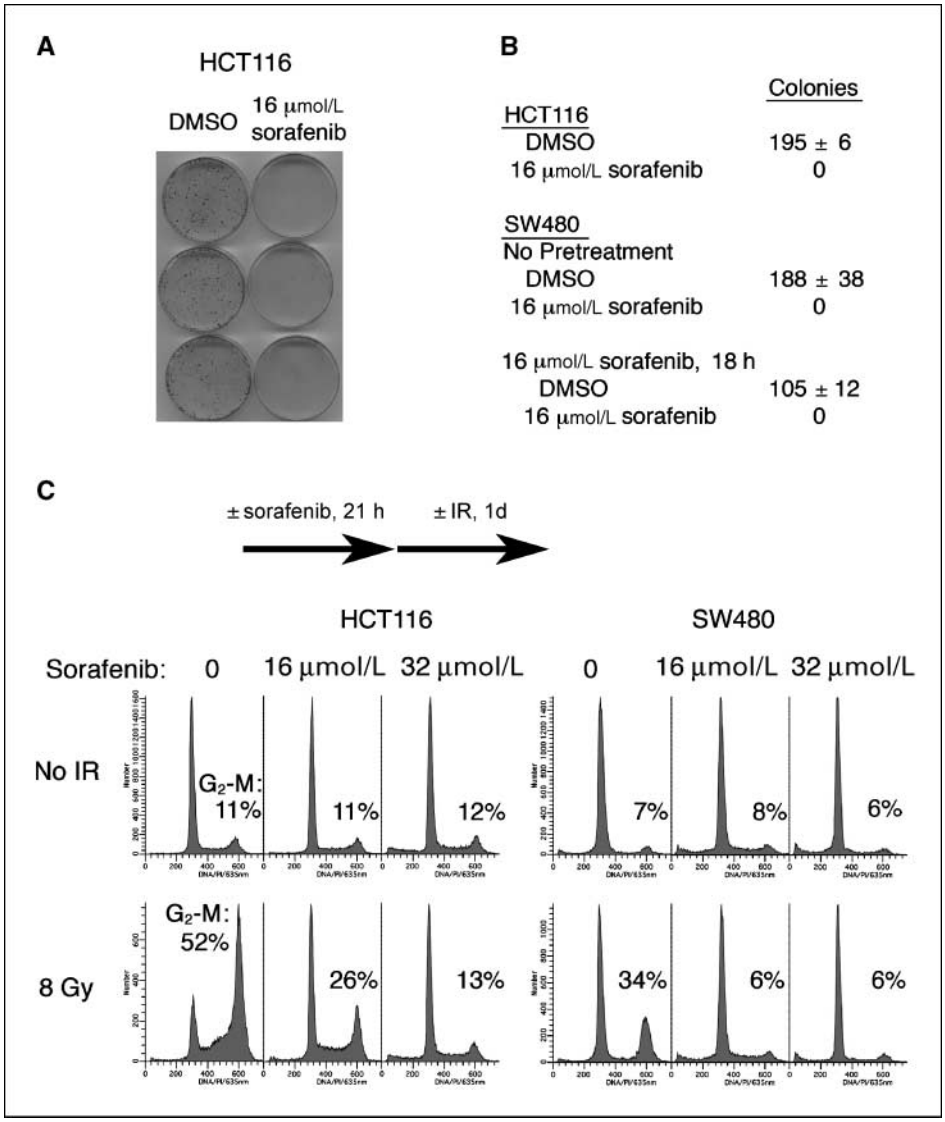

Figure 1. Sorafenib inhibits colony formation and prevents accumulation of irradiated cells in G_2-M. *A* and *B,* HCT116 and SW480 cells (400 per plate; $n = 3$) were allowed to grow in either DMSO (0.05%) or 16 μmol/L sorafenib for 10 to 14 d and colonies >50 cells were counted. Pretreatment of SW480 cells with 16 μmol/L sorafenib for 18 h decreased plating efficiency by 44% ($P = 0.02$). *C,* HCT116 (*top*) or SW480 (*bottom*) cells were grown to 70% confluence and then treated with either DMSO (0.05%) or sorafenib and incubated for 21 h. Cells were either irradiated with 8 Gy or mock treated and incubated for an additional 24 h. Adherent cells treated with trypsin to detach were stained with propidium iodide and analyzed by flow cytometry. The percentage of cells with 4N DNA content (G_2-M) is listed.

and DMEM (Calu-6, MCF-7, RCC-4, SAOS-2, SK-Mel-2, SK-Mel-5, 786-0, WT2, WM793B, and 293T). HCT116-Luc cells were created by infecting HCT116 cells with a retrovirus encoding firefly luciferase under puromycin selection, and pooled clones were used for the *in vivo* bioluminescence xenograft experiments. Glioblastoma multiforme lines were obtained from the University of California at San Francisco Brain Tumor Research Center Tissue Bank (U-343, SF-268, and SF-767) and cultured in DMEM. Except where serum-free conditions are indicated, complete medium is defined as the appropriate medium supplemented with 10% fetal bovine serum, penicillin (100 units/mL), and streptomycin (100 mg/mL). Human umbilical vein endothelial cells were obtained from Cambrex and cultured in EGM-2 medium. Cells were cultured at 37°C in humidified 5% CO_2/95% air.

Synchronization. Exponentially growing cells were serum starved for 24 h (0% serum), then grown in the presence of 10% serum and aphidicolin (2 μg/mL) for 16 h, and then released into freshly added serum-containing medium without aphidicolin.

MTT assay. Cells were plated into 96-well plates (2,000 per well) in 100 μL of serum-containing medium and allowed to grow for 1 day. An additional 100 μL of serum-containing medium with various concentrations of sorafenib were added to yield final concentrations ranging from 125 nmol/L to 32 μmol/L. After 3 days, 20 μL of 5 mg/mL MTT were added and incubated for 3 h. The supernatant was discarded, the precipitate was dissolved in 200 μL DMSO, and plates were read with a microplate reader at 570 nm.

Colony formation assays. Cells were treated with trypsin to detach, counted, and plated (400 per plate) into 60-mm dishes with either 0.05% DMSO or 16 μmol/L sorafenib and allowed to grow for 10 to 14 days. Cells were stained and colonies containing ≥50 cells were counted. In the pretreatment experiment, cells were pretreated with 16 μmol/L sorafenib for 18 h before trypsinization.

Cell cycle analysis. Floating and adherent cells were collected, fixed, and stained with propidium iodide. Flow cytometry was done using a Beckman Coulter Elite Epics sorter. The percentage of hypodiploid cells (sub-G_1) was used to quantify dead cells in apoptosis assays.

Tumor xenograft implantation in nude mice. Female NCR-*nu/nu* mice were obtained from Taconic. Experiments were carried out in accordance with the University Institutional Animal Care and Use Committee guidelines using an approved protocol. At 5 to 7 weeks of age, mice were injected with 2.8×10^6 HCT116-Luc cells suspended in 100 μL Matrigel (BD Collaborative Research) solution in the bilateral posterolateral flanks.

Irradiation. Human tumor cells were irradiated with a Mark I cesium irradiator (J.L. Shepherd) at a dose rate of 0.8 Gy/min. Tumor-bearing mice were irradiated with a 250 kV orthovoltage irradiator (Philips RT 250)

through a 0.2-mm copper filter. The source-to-skin distance was 30 cm. Lead was used to shield normal tissues where possible. Alternately, tumor-bearing mice were irradiated with a 6 MV linear accelerator (Varian 6/100) with 1 cm of bolus of tissue-equivalent material to allow for dose buildup. The dose rate was 2.0 Gy/min with a source-to-bolus distance of 100 cm. Collimators were used to shield normal tissues where possible.

Tumor regrowth delay. Tumor-bearing mice were treated with various schedules of sorafenib and fractionated radiation. Tumors were measured with calipers in two perpendicular diameters (a and b), and the volume was calculated as $V = [(a + b) / 2]^3 / 2$. Absolute growth delay (AGD) was defined as the time required from day 0 (first day of radiation) for the average relative tumor volume to triple.

Bioluminescence imaging. Tumor-bearing mice were imaged twice weekly using the Xenogen *In vivo* Imaging System. Mice were subjected to imaging within 15 to 30 min after i.p. injection of D-luciferin (5 mg/mouse) under anesthesia with i.p. ketamine/xylazine.

Western blotting. Cells were lysed on ice in reducing Laemmli sample buffer. Samples were boiled for 10 min, clarified by centrifugation, and stored at −80°C. Samples containing equal amounts of total protein were separated on NuPAGE 4% to 12% Bis-Tris gels and transferred to polyvinylidene difluoride membranes (Invitrogen). Immunoblotting was done with rabbit polyclonal anti-Mcl-1, anti-Rb (1:2,000), anti-phosphorylated Rb (S807/811 and S795; 1:1,000; Cell Signaling Technology), mouse anti-cyclin D1 (1:500; Calbiochem), mouse anti-p27 (1:500; Santa Cruz Biotechnology), mouse anti-p21 (1:250; Calbiochem), and mouse anti-Ran (1:5,000; BD PharMingen). Primary antibodies were detected using horseradish peroxidase–conjugated secondary antibodies and chemiluminescent substrates (Amersham Biosciences). For Ran detection, fluorochrome-conjugated secondary antibodies (1:5,000) were used and detected by IR scanning dosimetry using a Li-COR Odyssey Scanner.

Radiation survival studies. Cells were counted and variable numbers ranging from 200 to 20,000 were plated in 60-mm dishes and allowed to attach before irradiation. Colonies containing ≥50 cells were stained and counted at 2 weeks after irradiation. The surviving fraction was determined as the total number of colonies formed divided by the total number of cells plated multiplied by the plating efficiency, as determined in unirradiated cells in the presence or absence of drug exposure. Each point on the survival curve represents the mean surviving fraction from at least three replicates ± SD.

The addition of sorafenib in relation to time of irradiation was carried out according to three different sequences. (*a*) Short pretreatment: DMSO or sorafenib was added after cells were attached and 2 to 3 h before irradiation and medium was changed after an additional 24 h following irradiation. (*b*) Long pretreatment: cells were treated with DMSO or sorafenib for 24 h, trypsinized and counted, and then plated in the presence of drug. The medium was replaced after an additional 24-h incubation following radiation. (*c*) Posttreatment: DMSO or sorafenib was added within 2 to 3 min following radiation and medium was changed at 3 days following radiation.

Results

Sorafenib has broad-spectrum antigrowth activity against multiple human tumor cell lines and endothelial cells. Several studies have shown antiproliferative and proapoptotic activity of sorafenib using short-term assays in multiple cell lines, including colon (6), pancreas (6), melanoma (7, 8), leukemia (9, 10), thyroid (11), malignant glioma (12), lung (13), breast (13), and cholangiocarcinoma cell lines (9). Although sorafenib showed activity in these multiple studies, we sought to establish the relative sensitivities using a simple assay (MTT) in a panel of tumor cell lines derived from different tissues and to begin investigating the underlying mechanisms for growth inhibition. Viability following a 3-day treatment with varying concentrations of sorafenib (125 nmol/L to 32 μmol/L) was measured by the MTT assay, and the IC_{50}s are

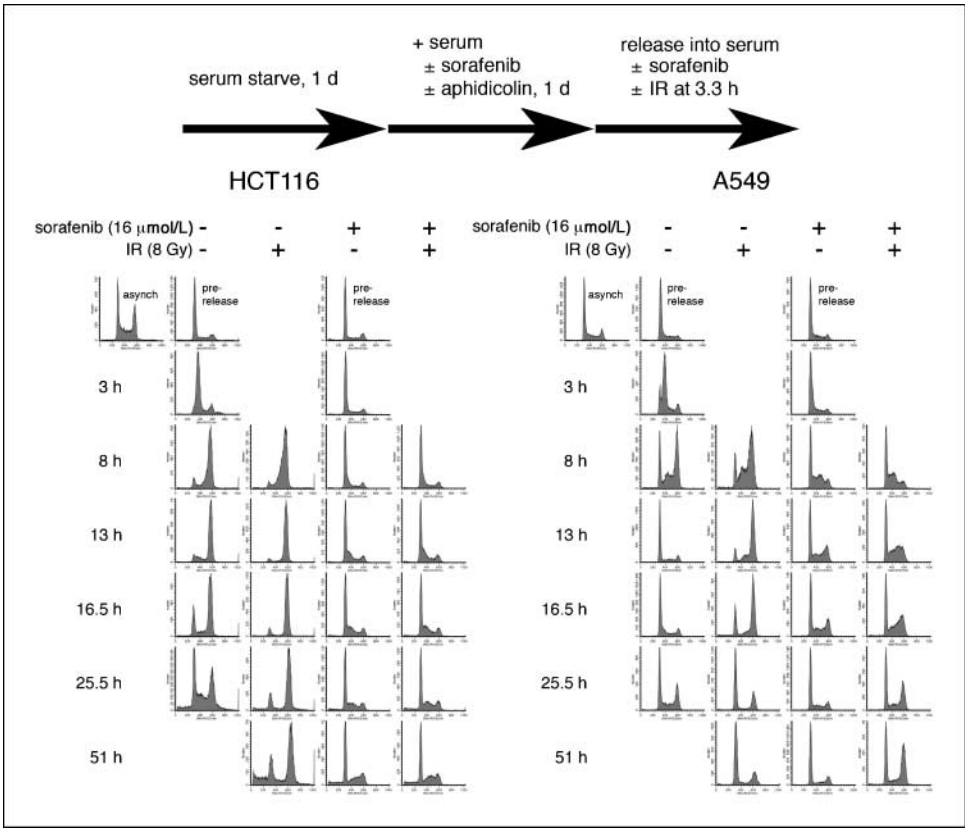

Figure 2. Sorafenib prevents synchronized, irradiated cells from reaching G_2-M by slowing cell cycle progression. HCT116 (*left*) or A549 (*right*) cells were plated at 10,000 per well into six-well plates and grown for 3 d. Cells were synchronized by serum starvation for 24 h followed by replacing the medium with serum-containing medium with aphidicolin (2 μg/mL) and either DMSO (0.1%) or sorafenib (16 μmol/L) for 16 h. Cells were released into fresh serum-containing medium with either DMSO (0.1%) or sorafenib (16 μmol/L). Cells were irradiated with 8 Gy or mock treated 3.3 h following release. Floating and adherent cells were harvested at various time points, stained with propidium iodide, and analyzed by flow cytometry.

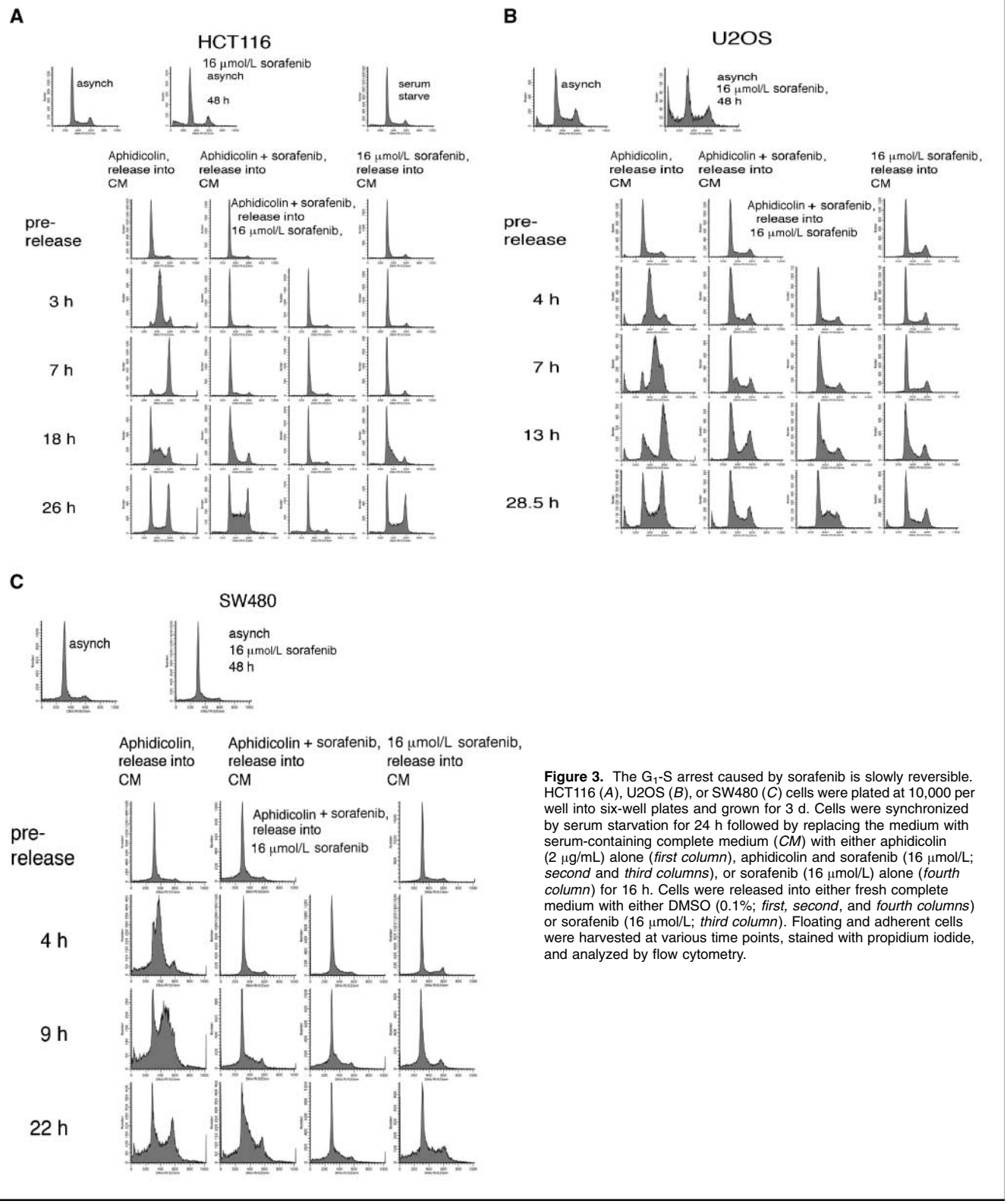

Figure 3. The G_1-S arrest caused by sorafenib is slowly reversible. HCT116 (*A*), U2OS (*B*), or SW480 (*C*) cells were plated at 10,000 per well into six-well plates and grown for 3 d. Cells were synchronized by serum starvation for 24 h followed by replacing the medium with serum-containing complete medium (*CM*) with either aphidicolin (2 μg/mL) alone (*first column*), aphidicolin and sorafenib (16 μmol/L; *second* and *third columns*), or sorafenib (16 μmol/L) alone (*fourth column*) for 16 h. Cells were released into either fresh complete medium with either DMSO (0.1%; *first, second*, and *fourth columns*) or sorafenib (16 μmol/L; *third column*). Floating and adherent cells were harvested at various time points, stained with propidium iodide, and analyzed by flow cytometry.

listed in Supplementary Table S1. There was little variation in sensitivity to sorafenib with IC_{50}s ranging from 5 to 15 μmol/L, which approximates clinically achievable serum concentrations (14) and is in a similar range where apoptosis has been observed (8–10). Growth-inhibitory effects have been observed at lower concentrations in the nanomolar to low micromolar range in melanoma and thyroid cell lines (7, 11), but IC_{50}s ranging from 5 to 15 μmol/L were observed in malignant glioma cell lines (12).

Others have found differences in sensitivity in melanoma cell lines. Molhoek et al. (7) found that cell lines with mutant B-Raf (V600E) were more sensitive to sorafenib in a growth inhibition assay; however, the differences observed in sorafenib-dependent apoptosis in three different melanoma lines were not dependent of B-Raf mutational status (A375 cells are more resistant than A2058 cells; ref. 8). The minor difference observed in the melanoma cell lines that we tested similarly did not follow B-Raf mutation status (Supplementary Table S1).

To evaluate the combination of sorafenib and radiation, we evaluated the effects of duration of sorafenib exposure on colony survival. Long-term colony formation assays with 16 μmol/L sorafenib in HCT116 and SW480 cells resulted in complete inhibition of colony formation (Fig. 1*A* and *B*). However, pretreatment for a limited

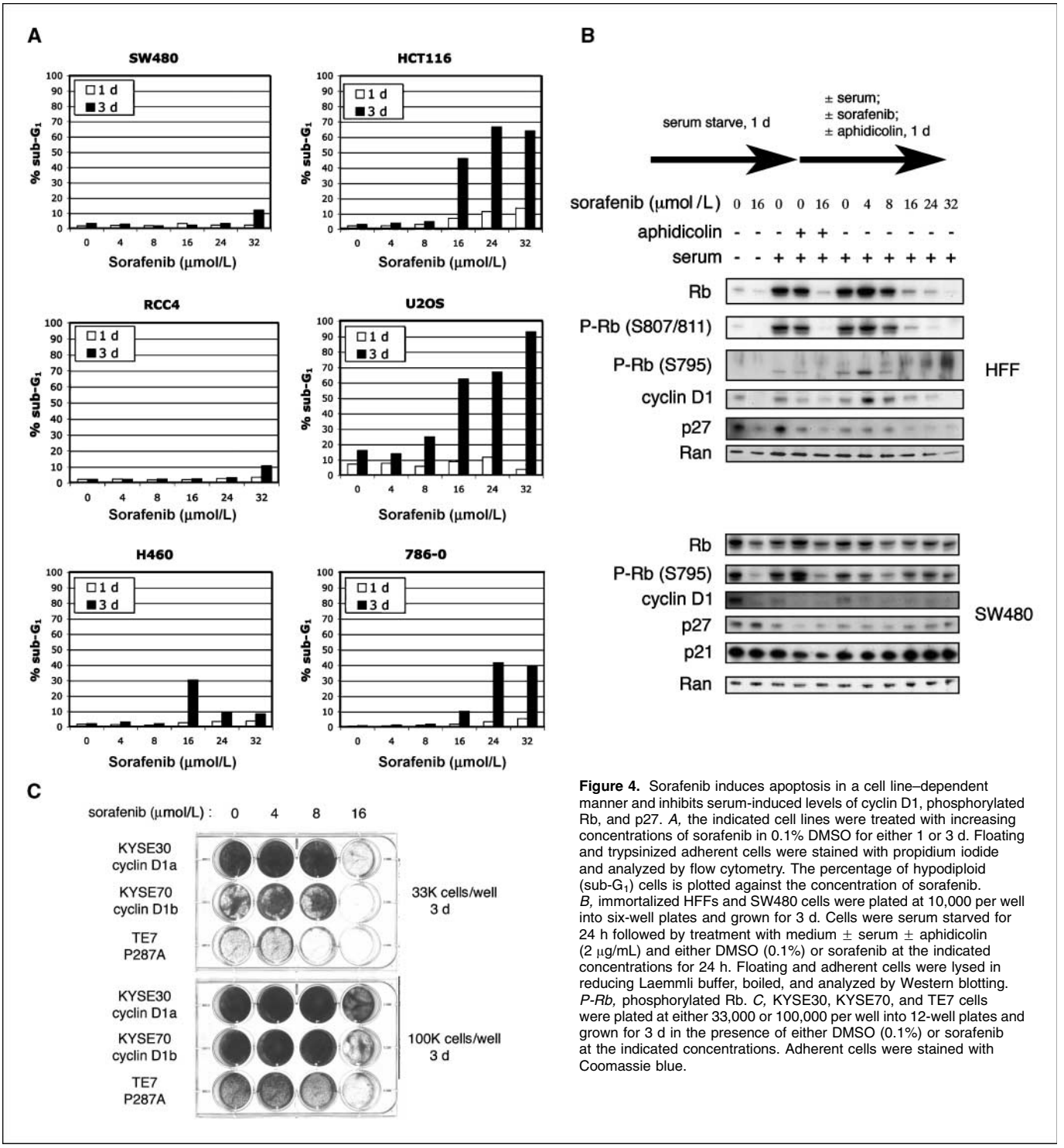

Figure 4. Sorafenib induces apoptosis in a cell line–dependent manner and inhibits serum-induced levels of cyclin D1, phosphorylated Rb, and p27. *A,* the indicated cell lines were treated with increasing concentrations of sorafenib in 0.1% DMSO for either 1 or 3 d. Floating and trypsinized adherent cells were stained with propidium iodide and analyzed by flow cytometry. The percentage of hypodiploid (sub-G_1) cells is plotted against the concentration of sorafenib. *B,* immortalized HFFs and SW480 cells were plated at 10,000 per well into six-well plates and grown for 3 d. Cells were serum starved for 24 h followed by treatment with medium ± serum ± aphidicolin (2 μg/mL) and either DMSO (0.1%) or sorafenib at the indicated concentrations for 24 h. Floating and adherent cells were lysed in reducing Laemmli buffer, boiled, and analyzed by Western blotting. *P-Rb,* phosphorylated Rb. *C,* KYSE30, KYSE70, and TE7 cells were plated at either 33,000 or 100,000 per well into 12-well plates and grown for 3 d in the presence of either DMSO (0.1%) or sorafenib at the indicated concentrations. Adherent cells were stained with Coomassie blue.

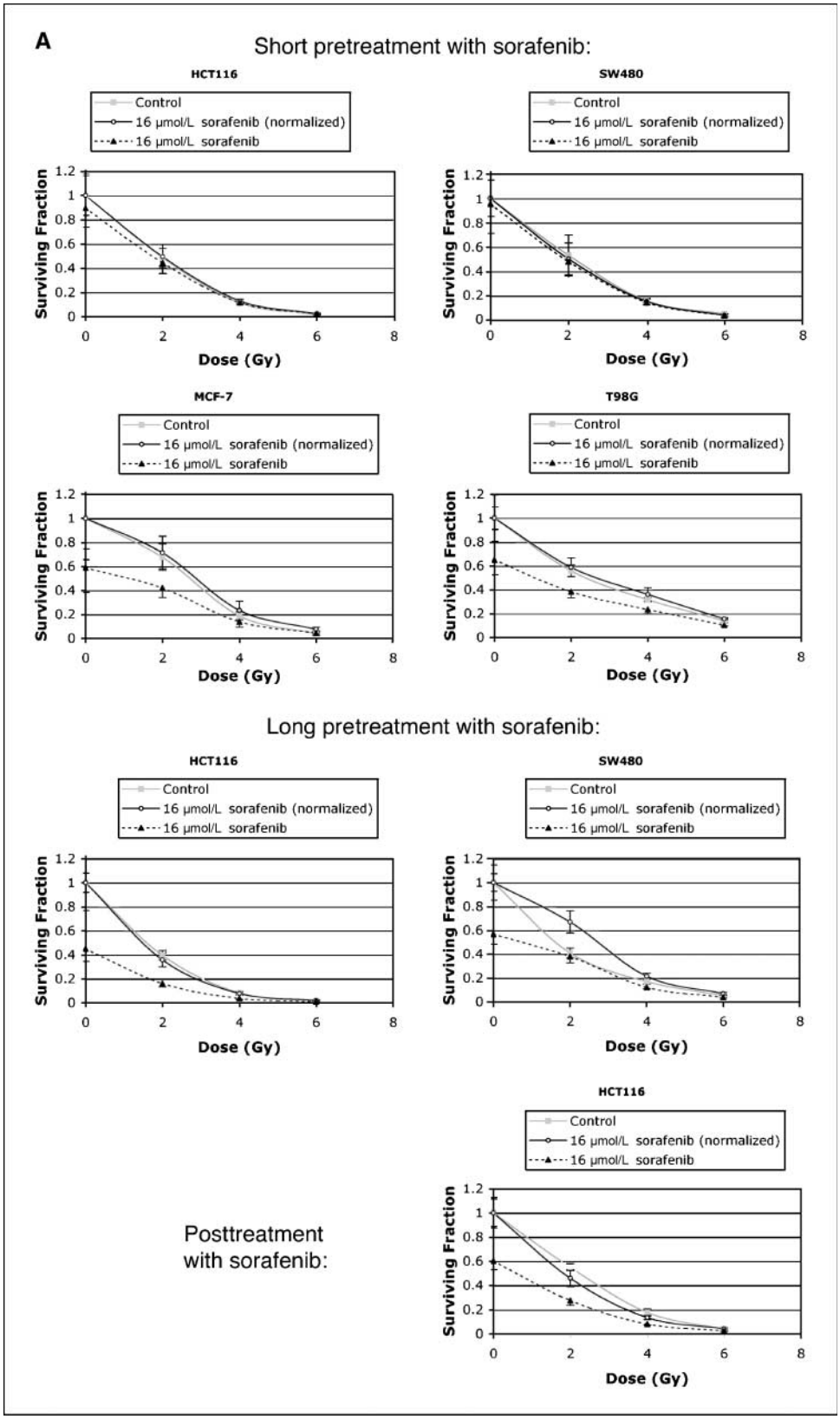

Figure 5. Sorafenib decreases the number and size of surviving colonies but does not alter the shape of the radiation dose-response curve. *A, top,* the indicated cell lines were treated with either 0.05% DMSO or 16 μmol/L (8 μmol/L for WM793B) sorafenib 2 to 3 h before irradiation. The medium was replaced after 24 h (or 48 h for WM793B). *Middle,* cells were treated with either 0.05% DMSO or 16 μmol/L sorafenib 24 h before irradiation, and after counting, cells were plated and allowed to attach in the presence of the drug before irradiation. The medium was replaced after an additional 24 h following irradiation. *Bottom,* cells were plated and irradiated, and within 30 min, medium was replaced with either 0.05% DMSO or 16 μmol/L sorafenib. Medium was replaced after 2 d. *Points,* surviving fractions are plotted against radiation dose (n = 3–6); *bars,* SD.

period with sorafenib reduced plating efficiency by 44% in SW480 cells (Fig. 1*B*). Thus, sorafenib is a potent inhibitor of colony formation in long-term colony-forming assays, but short treatment at a relatively high dose can be used in this assay to assess for radiosensitivity as described later. These results show a potent growth-inhibitory effect of sorafenib toward multiple tumor cell lines, but the underlying mechanism(s), which includes cell cycle arrest, apoptosis, or senescence, remained to be elucidated.

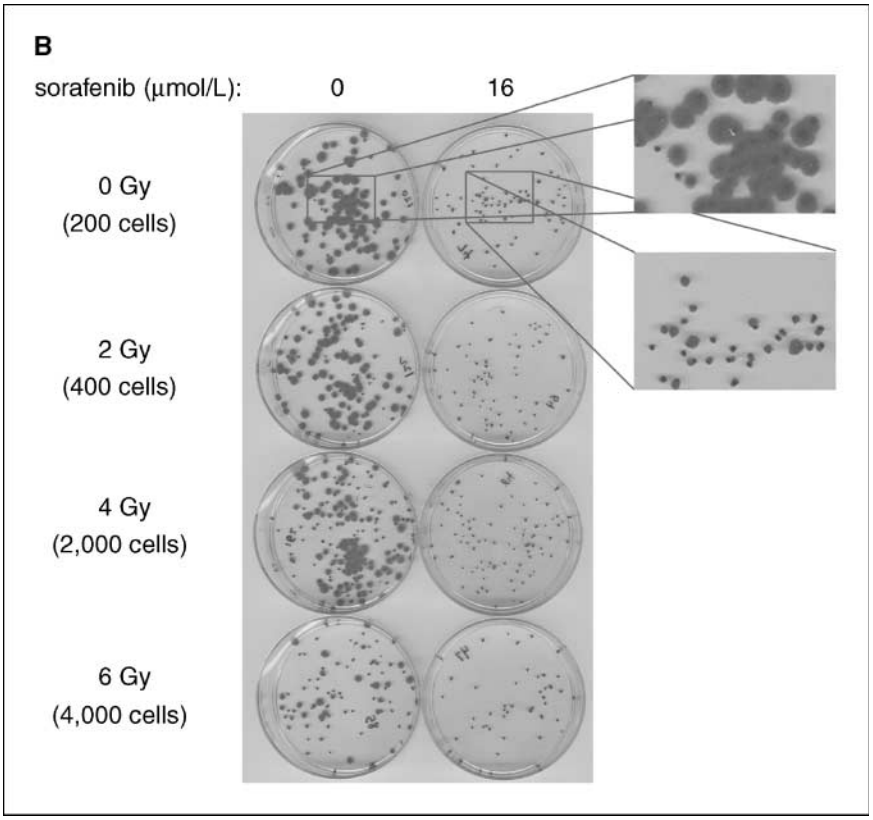

Figure 5 *Continued. B,* counted plates from *A*, *bottom*, show that sorafenib-treated HCT116 cell colonies are much smaller.

Sorafenib prevents accumulation of irradiated cells in G_2-M. To evaluate the effects of sorafenib on cell cycle phase distribution, we treated HCT116 and SW480 with increasing doses of sorafenib (Fig. 1*C, top*). Sorafenib up to 32 μmol/L had no apparent effect on cell cycle distribution of these cells. To further evaluate the cell cycle effects, we investigated the effects of sorafenib on unsynchronized, irradiated cells. To determine whether sorafenib could affect radiation-induced cell cycle accumulation in G_2-M, we pretreated cells with sorafenib for 24 h and then radiated cells with 8 Gy. After 24 h, cells were analyzed by flow cytometry. Interestingly, whereas sorafenib had no effect on unsynchronized cell cycle distribution, there was a profound effect on G_2-M accumulation (Fig. 1*C, bottom*).

We evaluated the effects of sorafenib on the cell cycle distribution of several other tumor cell lines (Supplementary Fig. S1). Consistent with the results in Fig. 1*C*, in the majority of tumor cell lines ($Bax^{-/-}$ HCT116, HT29, SKOV3, and H460), there was no apparent effect on cell cycle distribution following exposure to sorafenib. In contrast, PC3 cells exhibited a G_1 arrest similar to that observed in T98G malignant glioma cells (12). Other lines (HeLa, Calu-6, and U2OS) accumulated in S and G_2 (Supplementary Fig. S1). The ability of sorafenib to perturb the cell cycle may be related to inhibition of Raf kinase; however, the pleomorphic phenotype may be related to inhibition of other kinases in different cell lines.

The blockade of irradiated cells in G_2-M by sorafenib in Fig. 1*C* may be explained in one of two ways: (*a*) cells may have accumulated at earlier phases of the cell cycles, preventing their entry into G_2-M, or (*b*) sorafenib may have suppressed the G_2-M checkpoint, allowing irradiated cells to exit mitosis. Based on the results in Fig. 1*C*, we observed no obvious accumulation in G_1 or S in HCT116 and SW480 cells, thereby favoring the second explanation; however, we further tested these possibilities.

Kinetic analysis of synchronized cells reveals that sorafenib slows progression through S phase to delay G_2-M accumulation of irradiated cells. To assess whether reduced accumulation of irradiated cells in G_2-M following sorafenib treatment is due to blockade of the G_2-M checkpoint or prevention of cell cycle progression, cell synchronization studies were done. In addition to HCT116 cells, A549 cells, which have a robust and p53-independent G_2-M checkpoint, were studied (15, 16). We blocked HCT116 and A549 cells at the G_1-S boundary using serum starvation followed by refeeding with serum-containing medium with aphidicolin. As shown in Fig. 2, release from aphidicolin resulted in progressive accumulation of cells in S and G_2-M by 3 to 8 h and this was followed by exit from mitosis by 25 h in HCT116 or earlier (by 13 h) in A549 cells. Exposure to 8 Gy resulted in delayed exit from G_2-M in both HCT116 and A549 cells, consistent with the expected checkpoint activation. In contrast to controls, sorafenib alone prevented cells from progressing through S phase following aphidicolin release. The combination of sorafenib and radiation seemed to limit the accumulation of irradiated cells in G_2-M. Few synchronized HCT116 cells treated with both sorafenib and radiation even made it to G_2-M (Fig. 2, *left*), which likely accounts for the lack of G_2-M accumulation observed in Fig. 1*C*. A549 cells were slightly more resistant to the sorafenib-induced cell cycle slowing, and consequently, more cells treated with both sorafenib and radiation reached G_2-M (Fig. 2, *right*). Even in the presence of sorafenib, irradiated A549 cells exhibited a G_2-M checkpoint, which argues against the hypothesis that sorafenib inhibits this checkpoint.

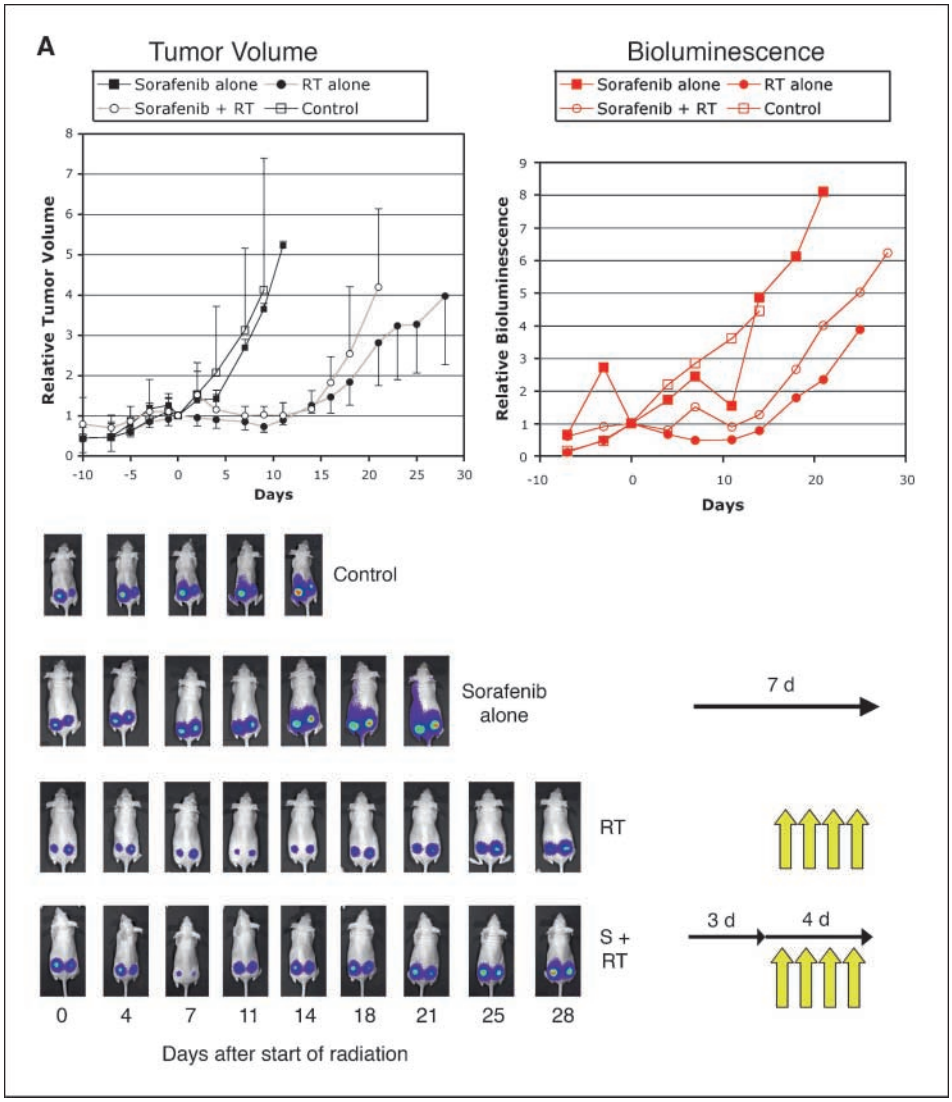

Figure 6. Sequential treatment with radiation followed by sorafenib is more effective than concurrent treatment of HCT116 human colon tumor xenografts. *A,* luciferase-expressing HCT116 tumors (two tumors per mouse) were grown on the backs of nude mice to an average size of 64 ± 42 mm^3. Mice were either untreated (control, n = 10 tumors) or treated with 7 d of daily sorafenib (60 mg/kg/d i.p.) from day −3 to day +3 (sorafenib alone, n = 10 tumors), 4 d of daily radiation therapy (300 cGy/fraction) from day 0 to day +3 [radiation (*RT*) alone, n = 8 tumors], or 7 d of daily sorafenib (60 mg/kg/d i.p.) from day −3 to day +3 with 4 d of daily radiation (300 cGy/fraction) from day 0 to day +3 with sorafenib given 75 min before daily radiation (sorafenib + radiation, n = 8 tumors). Tumor regrowth was measured by caliper measurements and luciferase bioluminescence. Tumor volumes from each tumor were normalized to day 0 (first day of radiation). *Points,* mean relative tumor volumes over time; *bars,* SD. Bioluminescence from each tumor was normalized to day 0, and mean relative bioluminescence over time is shown (error bars omitted for clarity). Photographs with color wash bioluminescence overlay are shown from a representative mouse from each group over time.

Sorafenib-induced G_1-S delay is reversible. To test whether sorafenib-induced G_1-S accumulation (Fig. 2) represented a bona fide arrest, we synchronized cells with sorafenib alone or with aphidicolin followed by release into drug-free medium.

As in Fig. 2, aphidicolin-synchronized HCT116 cells refed with complete medium reached G_2-M by 7 h and reentered G_1 at 18 h (Fig. 3*A, first column*). However, when HCT116 cells were synchronized with aphidicolin and sorafenib, and then released into complete medium, it took at least 26 h to reach G_2-M, indicating a persistent delay, even in the absence of drug (Fig. 3*A, second column*). If synchronized cells were maintained in sorafenib, there was little progression (Fig. 3*A, third column*). If serum-starved HCT116 cells were treated with sorafenib and aphidicolin (Fig. 3*A, fourth column*), there was enrichment at G_1 or G_1-S compared with asynchronous cells (Fig. 3*A, top row, left*). When "sorafenib-synchronized" cells were released into drug-free complete medium, cell cycle progression was significantly delayed, with cells entering S phase between 7 and 18 h and only reaching G_2-M at 26 h (Fig. 3*A, fourth column*). These results indicate cells were delayed in G_1 or G_1-S and that the delay is slowly reversible. Similar observations were made with U2OS osteosarcoma and SW480 colon cancer cells (Fig. 3*B* and *C*), although there were differences. In the sustained presence of sorafenib, a larger percentage of synchronized U2OS cells progressed into S phase (Fig. 3*B, third column*) compared with HCT116 cells continuously exposed to sorafenib. This may indicate a difference in sensitivity to sorafenib-induced cell cycle delay despite the observation that the IC_{50}s for these cell lines were similar as measured by the MTT assay (Supplementary Table S1). Together, these results show that sorafenib delays cell cycle progression in a variety of cell lines.

Sorafenib induces apoptosis in a cell line–dependent manner. Sorafenib-induced cell cycle delay could account for the activity in the MTT assay and colony formation assay. However, it was possible that sorafenib caused cell death in addition to growth delay, which was indicated by the presence of hypodiploid populations, especially at later time points in Figs. 2 and 3. To determine if the activity of sorafenib in the viability and colony formation assays was due to cytotoxicity or cytostasis, we further evaluated a panel of cell lines for cell death on exposure to sorafenib by sub-G_1 analysis (Fig. 4*A*). Sorafenib induced death in a concentration-dependent manner in HCT116, U2OS, and 786-0 cells, whereas minimal cell death was observed in SW480, RCC-4,

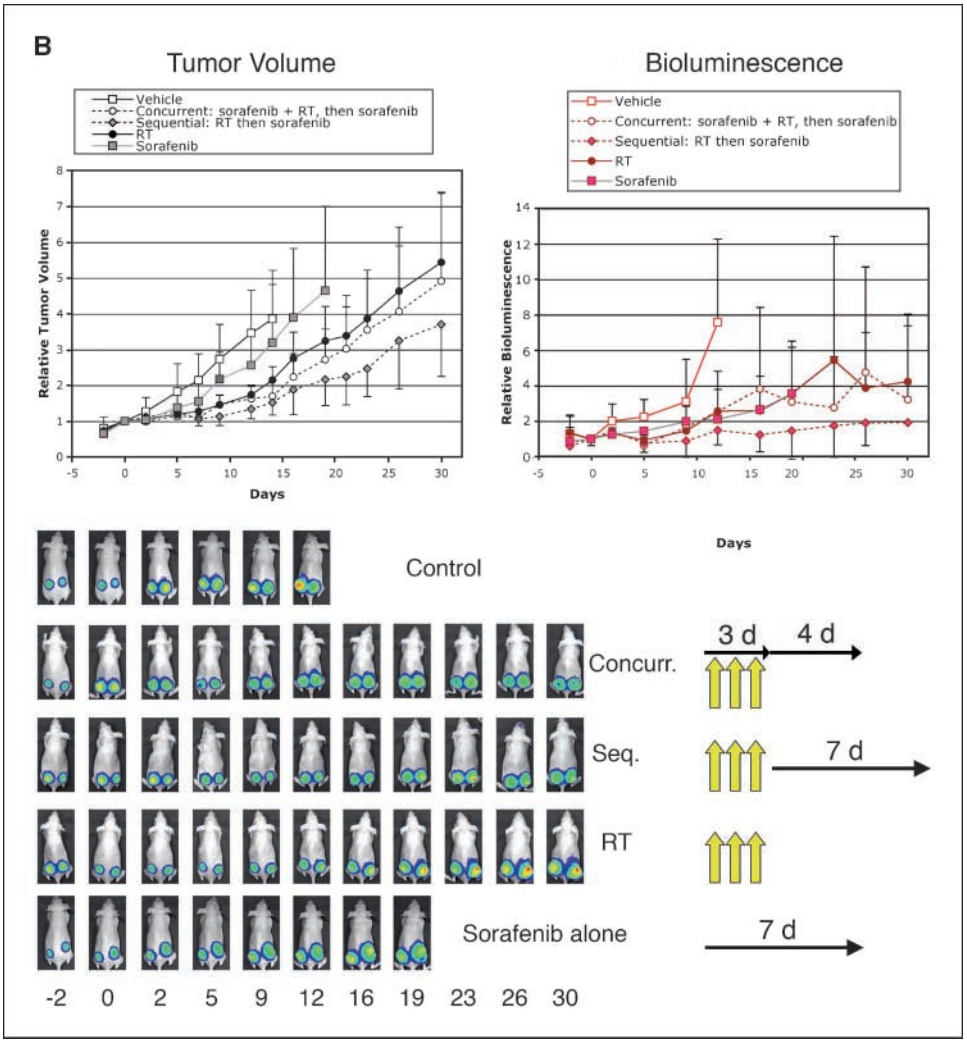

Figure 6 *Continued. B,* luciferase-expressing HCT116 tumors (two tumors per mouse) were grown on the backs of nude mice to an average size of 287 ± 98 mm^3. Mice were treated with either 7 d of vehicle (vehicle, $n = 10$ tumors), 7 d of daily sorafenib (60 mg/kg/d i.p.) from day 0 to day +6 with 3 d of daily radiation (250 cGy/fraction) from day 0 to day +2 with sorafenib given 12 h before daily radiation (concurrent sorafenib + radiation and then sorafenib, $n = 8$ tumors), 3 d of daily radiation (250 cGy/fraction) from day 0 to day +2 followed by 7 d of daily sorafenib (60 mg/kg/d i.p.) from day +3 to day +9 (sequential radiation and then sorafenib, $n = 8$ tumors), 3 d of daily radiation (250 cGy/fraction) from day 0 to day +2 (radiation alone), or 7 d of daily sorafenib (60 mg/kg/d i.p.) from day 0 to day +6 (sorafenib alone, $n = 10$ tumors). Tumor regrowth was measured as in *A*. *Bars,* SD.

and H460 cells. This difference in susceptibility to drug-induced apoptosis did not correlate with p53 status or activated Ras mutational status. The observation that sorafenib only induces apoptosis in certain cell lines points to the importance of the effect of sorafenib on the cell cycle.

Serum-induced levels of cyclin D1, phosphorylated Rb, and p27 are inhibited by sorafenib. To further characterize the observed cell cycle delay, we examined the expression of cell cycle regulatory proteins in synchronized cells treated with sorafenib. Cells were serum starved and then either synchronized with aphidicolin or released into serum ± sorafenib (Fig. 4*B*). In human foreskin fibroblasts (HFF) and SW480 cells, treatment with sorafenib decreased levels of cyclin D1. Decreased cyclin D1 may result in decreased cyclin D/cyclin-dependent kinase 2–dependent Rb phosphorylation. Although sorafenib apparently blocks Rb phosphorylation at S807/811 and S795 in both HFF and SW480 cells, sorafenib also decreased total levels of Rb, especially in fibroblasts. Blockade of the mitogen-activated protein kinase (MAPK) pathway may increase levels of p27, but sorafenib did not reliably increase p27 levels. The observed changes in these proteins are consistent with cell cycle perturbation but not complete arrest. If hypophosphorylated Rb and p27 had accumulated with concurrent loss of cyclin D1, one would predict a G_1 arrest. However, sorafenib decreased levels of cyclin D1, total Rb, and phosphorylated Rb consistent with G_1 delay and preserved ability to slowly enter S phase. Why sorafenib-treated cells are delayed in S phase is unknown.

To test whether decreased cyclin D1 is responsible for growth inhibition by sorafenib, cell lines defective in cyclin D1 degradation were tested (Fig. 4*C*). KYSE30 cells express cyclin D1a, which is normally degraded and served as a control (17). KYSE70 cells predominantly express cyclin D1b (17), a splice variant resistant to degradation. Similarly, TE7 cells have mutant cyclin D1, P287A, which cannot be phosphorylated on T286, a signal for degradation (18). Both KYSE70 and TE7 cells have cyclin D1 isoforms that are resistant to degradation and would be expected to be resistant to sorafenib if reduction of cyclin D1 were the key mechanism of action. As shown in Fig. 4*C*, even when cyclin D1 is stabilized, the cells are sensitive to growth inhibition by sorafenib, suggesting that targets other than cyclin D1 are important. It is also possible that sorafenib targets cyclin D1 synthesis. In either case, these data suggest that sorafenib would be effective even in cancers with stabilized cyclin D1.

Sorafenib decreases the number and size of surviving colonies but does not alter the shape of the radiation dose-response curve. The effects of cell cycle–active agents on

radiosensitivity are complex, but it is generally accepted that cells in G_1 and early S phase are more radiosensitive than those in late S (19). Because sorafenib inhibits radiation-induced G_2-M accumulation, most likely by causing delays in progression through earlier phases of the cell cycle, we tested sorafenib in radiation survival assays. The schedule of sorafenib and radiation treatment was varied in *in vitro* radiation survival assays (Fig. 5*A*). To test cell cycle phase-independent effects, cells were treated for 2 to 3 h with sorafenib before radiation and then removed 1 to 2 days after radiation (Fig. 5*A, top*). Although treatment with sorafenib reduced plating efficiency in some cell lines, this short pretreatment did not affect the relative surviving fraction. To test the effect of cell cycle accumulation, cells were pretreated with sorafenib for 24 h before radiation followed by continued exposure to sorafenib for an additional 24 h (Fig. 5*A, middle*). Longer pretreatment reduced the plating efficiency of HCT116 and SW480 cells but did not affect the relative surviving fraction. Finally, treatment with sorafenib for 48 h after radiation decreased the plating efficiency but did not radiosensitize the cells (Fig. 5*A, bottom*). Together, these results contrast the observation that antisense RNA to Raf-1 radiosensitizes but are consistent with observations that inhibitors of MAPK/extracellular signal-regulated kinase kinase (MEK), the kinase downstream of Raf, have not been shown to radiosensitize (20). Although sorafenib did not synergize with radiation as measured by normalized colony number, sorafenib treatment resulted in dramatically smaller colonies (Fig. 5*B*). Although colony-forming assays did not show synergy, it is possible that sorafenib may sensitize cells to radiation-induced apoptosis. Cancer cell lines that were either sensitive (HCT116 and U2OS) or resistant (SW480 cells) to sorafenib-induced apoptosis were tested for sensitization to radiation-induced apoptosis (Supplementary Fig. S2). None of these cell lines showed appreciable levels of radiation-induced apoptosis regardless of sorafenib pretreatment. Despite the apparent lack of synergy in these *in vitro* assays, it is possible that sorafenib could potentiate the radiation antitumor effect *in vivo*, as sorafenib is a multikinase inhibitor with antiangiogenic effects (21). This possibility was further tested.

Sorafenib enhances the antitumor effect of radiation in a schedule-dependent manner in human tumor xenografts. Because sorafenib is expected to have effects on the tumor microenvironment as a result of its antiangiogenic properties (21), we evaluated the ability of sorafenib to affect radiosensitivity in a nude mouse xenograft model. Luciferase-expressing HCT116 tumors were grown on the backs of nude mice, which were either not treated, treated with 7 days of sorafenib (60 mg/kg), radiated with four daily fractions of 300 cGy/fraction starting on day 0, or pretreated with 3 days of sorafenib followed by concurrent treatment with sorafenib administered 75 min before radiation treatments for 4 days. Tumor growth delay was monitored by tumor volume and tumor bioluminescence. As can be seen in Fig. 6*A*, sorafenib alone minimally increased the AGD from 6.7 to 7.7 days. Pretreatment followed by concurrent treatment with sorafenib resulted in more rapid regrowth (AGD, 18.8 days) than radiation alone (AGD, 21.9 days). In Fig. 6*B*, alternate sequences were tested, namely concurrent treatment with sorafenib and radiation for 3 days followed by sorafenib for 4 days (AGD, 20.8 days) or sequential treatment with 3 days of radiation followed by 7 days of sorafenib (AGD, 25.0 days). Compared with vehicle (AGD, 10.1 days), radiation alone for 3 days (AGD, 17.5 days), or sorafenib alone for 7 days (AGD, 13.4 days), sequential treatment delayed tumor growth the most as determined by tumor volume. As determined by relative tumor bioluminescence, the sequential schedule seemed to delay tumor regrowth the most, whereas concurrent treatment with radiation and sorafenib was no better than radiation alone (Fig. 6*B*). Thus, regardless of sequence, concurrent treatment with sorafenib is no better than radiation alone. Alternatively, sequential sorafenib treatment following radiation increases the effectiveness of either treatment alone. The effectiveness of sequential radiation following sorafenib treatment is unknown.

Discussion

We report the cell cycle and antitumor effects of a combination of sorafenib and radiation and establish the optimal schedule for coadministration *in vivo*. We unravel several previously unappreciated effects of sorafenib on cell growth inhibition, including a G_1-S cell cycle delay in synchronized cells, and effects on serum-stimulated cyclin D1 and Rb accumulation. Our studies highlight the importance of careful synchronization in delineating cell cycle effects. Sequential treatment with radiation followed by sorafenib had the greatest *in vivo* antitumor effect, showing the importance of treatment schedule. These results provide a rationale for combination treatment with sorafenib and radiation as well as a preferred schedule of administration.

Sorafenib is broadly active in multiple cell lines regardless of histology, Ras, or Raf mutational status. Although selected normal cell lines were sensitive to sorafenib *in vitro*, tumor-bearing patients and animals treated with sorafenib have tumor shrinkage with minimal toxicity, indicating that the therapeutic index is wide *in vivo*. In melanoma cell lines, mutant B-Raf (V600E) predicts sensitivity to MEK inhibitors (22) and sorafenib (7). Unlike Molhoek et al. (7) who used lower concentrations and a short (1 h) treatment time in a sensitive growth inhibition, we did not find that B-Raf mutational status affected sensitivity to sorafenib in the MTT assay. The MTT assay measures both cell growth and death, and others have shown that sorafenib-dependent apoptosis is not due to Raf mutational status, pointing to alternate targets in the determination of sorafenib sensitivity (8). Others have shown the importance of decreased Mcl-1 levels in sorafenib-dependent apoptosis (9, 10). We also found that sorafenib decreased Mcl-1 levels in most cell lines tested (Supplementary Data). Interestingly, we found that sorafenib-dependent apoptosis was cell line dependent but did not correlate with decreases in Mcl-1. The use of sorafenib to target Mcl-1 can help guide combination therapies. For example, it would be interesting to combine ABT-737 with sorafenib as down-regulation of Mcl-1 is synergistic with ABT-737, an inhibitor of Bcl-2 and Bcl-XL (23). Sorafenib may sensitize cells to the death receptor ligand tumor necrosis factor–related apoptosis-inducing ligand (24). Sorafenib has shown preclinical synergy with other "biological" antitumor agents, such as inhibitors of mammalian target of rapamycin (7), protein kinase Cδ (12), and the proteasome (13). Interestingly, sorafenib has shown synergy with SN-38, an active metabolite of CPT-11, but antagonism with other classic antineoplastic drugs, including paclitaxel, 5-fluorouracil (5-FU), and platinum-containing drugs (25, 26). The antagonism of sorafenib with platinum-containing compounds was hypothesized to be either from decreased uptake of the platinum drugs or an antagonistic effect on the cell cycle (25).

The effect of sorafenib on the cell cycle may in part be explained by inhibition of Raf kinase. Signaling through the MAPK pathway leads to expression of cyclin D1, phosphorylation of Rb, and ultimately progression through the G_1-S checkpoint. Targeted

inhibition of the MAPK pathway would be expected to lead to a G_1 block, but this was not consistently observed. We observed that sorafenib causes no obvious arrest in the majority of asynchronous cell lines but causes a G_1, S, or G_2 arrest in some cell lines. Consistent with a cell line–dependent effect, it has been observed that, in the glioblastoma cell line T98G, sorafenib causes a time- and concentration-dependent G_1 arrest with a decrease in cyclin D1 levels (12). A targeted MEK inhibitor, CI-1040, leads to a G_1 arrest of asynchronous cells with decreased levels of cyclin D1, but this occurs preferentially in cells with mutant B-Raf (22). It is possible that cell lines with mutant B-Raf would have a similar effect when treated with sorafenib. The effect of sorafenib on the cell cycle becomes most obvious when cells are synchronized or cotreated with an agent that causes cell cycle blockade, such as ionizing radiation. Heim et al. (25) found that sorafenib blocked the G_2 arrest induced by cisplatin as well as the G_1 arrest induced by oxaliplatin while decreasing levels of cyclin D1 and p21. The heterogeneous effects on cell cycle progression may be more consistent with multiple targets rather than mediated solely through Raf inhibition.

The *in vivo* antitumor effects of sorafenib combined with radiation yielded the surprising result that sequential treatment of sorafenib following radiation was superior to concurrent treatment. The effects of a radiosensitizing agent can be divided into intrinsic effects and microenvironmental effects. Based on colony formation assays, sorafenib and radiation cooperated to yield fewer and smaller colonies, but there was not true synergistic radiosensitization. There may have been balanced competing effects of antagonism due to cell cycle delay, allowing more time for repair of sublethal damage and sensitization through effects on potentially lethal damage repair. The latter may be expected from effects on survival pathways, such as Mcl-1, analogous to the radiosensitization caused by inhibitors of the phosphatidylinositol 3-kinase/Akt pathway (27). Effects on the tumor microenvironment are best tested with *in vivo* models. Agents that target tumor vasculature and angiogenesis are generally additive or supra-additive when combined with radiation (28). Although sorafenib has antiangiogenic activity, concurrent treatment with radiation was no better than radiation alone, whether it was given with a "run in" (Fig. 6*A*) or "run out" (Fig. 6*B*). It is possible that an antagonistic cell cycle effect counteracted any beneficial effect from antiangiogenesis or blocking of survival pathways. Clearly, both radiation and sorafenib treatment are effective antitumor treatments, which was noted *in vitro* by the decreased size of the sorafenib-treated colonies in the colony formation assays and *in vivo* by the observation that sequential treatment was effective. Although we found that the sequential schedule had more antitumor activity than radiation alone or concurrent treatment, the optimal schedule of sequential treatment remains an open question. Sorafenib treatment followed by radiation sequentially was not tested, and it would be of interest to compare this schedule with radiation first followed by sorafenib (Fig. 6*B*). It may be that sorafenib inhibition of angiogenesis following radiation was effective by inhibiting proliferation of endothelium damaged by radiation. Alternately, the antiangiogenic effect of pretreatment with sorafenib may be superior by improving tumor oxygenation and thus radiosensitivity, similar to what is observed with anti-VEGF antibody pretreatment (29).

This study establishes a preferred schedule for combining sorafenib with clinical radiotherapy. Based on our *in vivo* data, because sorafenib and radiation seem to have the greatest antitumor effect when administered in sequence, clinical trials with concurrent sorafenib and radiation are not warranted at this time. When the toxicities of sorafenib are considered (i.e., diarrhea and skin reactions), the safety of combination treatment with 5-FU–sensitized radiation for gastrointestinal malignancies should be cautiously studied. Sequential treatment with radiation and then sorafenib seems to be superior to concurrent treatment. In preoperative regimens with concurrent chemoradiation for gastrointestinal malignancies (i.e., rectal and esophageal cancer), there is usually a period of at least 4 weeks between chemoradiation and surgery. The window between chemoradiation and surgery may be an opportune time to introduce a targeted agent such as sorafenib that is well tolerated to maximize antitumor effect. We are developing a phase I/II trial in preoperative rectal adenocarcinoma with toxicity and pathologic complete response rate as primary end points.

Acknowledgments

Received 4/20/2007; revised 7/13/2007; accepted 7/20/2007.

Grant support: Radiological Society of North America; NIH grants CA75138, CA098101, and CA105008; and the Littlefield-AACR award for research on metastatic colon cancer.

The costs of publication of this article were defrayed in part by the payment of page charges. This article must therefore be hereby marked *advertisement* in accordance with 18 U.S.C. Section 1734 solely to indicate this fact.

References

1. Eisen T, Ahmad T, Flaherty KT, et al. Sorafenib in advanced melanoma: a phase II randomised discontinuation trial analysis. Br J Cancer 2006;95:581–6.
2. Eisen T, Ahmad T, Gore ME, et al. Phase I trial of BAY 43-9006 (sorafenib) combined with dacarbazine (DTIC) in metastatic melanoma patients. J Clin Oncol 2005;23:7508.
3. Flaherty KT, Brose M, Schuchter L, et al. Phase I/II trial of BAY 43-9006, carboplatin (C) and paclitaxel (P) demonstrates preliminary antitumor activity in the expansion cohort of patients with metastatic melanoma. J Clin Oncol 2004;22:7507.
4. Bankston D, Dumas J, Natero R, Riedl B, Monahan M, Sibley RA. Scaleable synthesis of BAY 43-9006: a potent Raf kinase inhibitor for the treatment of cancer. Organic Process Res Dev 2002;6:777–81.
5. Zhang L, Yu J, Park BH, Kinzler KW, Vogelstein B. Role of BAX in the apoptotic response to anticancer agents. Science 2000;290:989–92.
6. Wilhelm S, Chien DS. BAY 43-9006: preclinical data. Curr Pharm Des 2002;8:2255–7.
7. Molhoek KR, Brautigan DL, Slingluff CL, Jr. Synergistic inhibition of human melanoma proliferation by combination treatment with B-Raf inhibitor BAY43-9006 and mTOR inhibitor rapamycin. J Transl Med 2005;3:39.
8. Panka DJ, Wang W, Atkins MB, Mier JW. The Raf inhibitor BAY 43-9006 (sorafenib) induces caspase-independent apoptosis in melanoma cells. Cancer Res 2006;66:1611–9.
9. Yu C, Bruzek LM, Meng XW, et al. The role of Mcl-1 downregulation in the proapoptotic activity of the multikinase inhibitor BAY 43-9006. Oncogene 2005;24:6861–9.
10. Rahmani M, Davis EM, Bauer C, Dent P, Grant S. Apoptosis induced by the kinase inhibitor BAY 43-9006 in human leukemia cells involves down-regulation of Mcl-1 through inhibition of translation. J Biol Chem 2005;280:35217–27.
11. Salvatore G, De Falco V, Salerno P, et al. BRAF is a therapeutic target in aggressive thyroid carcinoma. Clin Cancer Res 2006;12:1623–9.
12. Jane EP, Premkumar DR, Pollack IF. Coadministration of sorafenib with rottlerin potently inhibits cell proliferation and migration in human malignant glioma cells. J Pharmacol Exp Ther 2006;319:1070–80.
13. Yu C, Friday BB, Lai JP, et al. Cytotoxic synergy between the multikinase inhibitor sorafenib and the proteasome inhibitor bortezomib *in vitro*: induction of apoptosis through Akt and c-Jun NH_2-terminal kinase pathways. Mol Cancer Ther 2006;5:2378–87.
14. Clark JW, Eder JP, Ryan D, Lathia C, Lenz HJ. Safety and pharmacokinetics of the dual action Raf kinase and vascular endothelial growth factor receptor inhibitor, BAY 43-9006, in patients with advanced, refractory solid tumors. Clin Cancer Res 2005;11:5472–80.

15. Giuliano KA, Chen YT, Taylor DL. High-content screening with siRNA optimizes a cell biological approach to drug discovery: defining the role of p53 activation in the cellular response to anticancer drugs. J Biomol Screen 2004;9:557–68.
16. Roussel E, Belanger MM, Couet J. G_2/M blockade by paclitaxel induces caveolin-1 expression in A549 lung cancer cells: caveolin-1 as a marker of cytotoxicity. Anticancer Drugs 2004;15:961–7.
17. Lu F, Gladden AB, Diehl JA. An alternatively spliced cyclin D1 isoform, cyclin D1b, is a nuclear oncogene. Cancer Res 2003;63:7056–61.
18. Benzeno S, Lu F, Guo M, et al. Identification of mutations that disrupt phosphorylation-dependent nuclear export of cyclin D1. Oncogene 2006;25: 6291–303.
19. Sinclair WK, Morton RA. X-ray and ultraviolet sensitivity of synchronized Chinese hamster cells at various stages of the cell cycle. Biophys J 1965;5:1–25.
20. Gupta AK, Bakanauskas VJ, Cerniglia GJ, et al. The Ras radiation resistance pathway. Cancer Res 2001;61: 4278–82.
21. Wilhelm SM, Carter C, Tang L, et al. BAY 43-9006 exhibits broad spectrum oral antitumor activity and targets the RAF/MEK/ERK pathway and receptor tyrosine kinases involved in tumor progression and angiogenesis. Cancer Res 2004;64:7099–109.
22. Solit DB, Garraway LA, Pratilas CA, et al. BRAF mutation predicts sensitivity to MEK inhibition. Nature 2006;439:358–62.
23. van Delft MF, Wei AH, Mason KD, et al. The BH3 mimetic ABT-737 targets selective Bcl-2 proteins and efficiently induces apoptosis via Bak/Bax if Mcl-1 is neutralized. Cancer Cell 2006;10:389–99.
24. Ricci MS, Kim S-H, Ogi K, et al. Repression of TRAIL-induced Mcl-1 and c-IAP2 expression by c-Myc or BAY 43-9006 (sorafenib) sensitizes resistant human cancer cells to TRAIL-induced death. Cancer Cell 2007; 12:66–80.
25. Heim M, Scharifi M, Zisowsky J, et al. The Raf kinase inhibitor BAY 43-9006 reduces cellular uptake of platinum compounds and cytotoxicity in human colorectal carcinoma cell lines. Anticancer Drugs 2005;16:129–36.
26. Heim M, Sharifi M, Hilger RA, Scheulen ME, Seeber S, Strumberg D. Antitumor effect and potentiation or reduction in cytotoxic drug activity in human colon carcinoma cells by the Raf kinase inhibitor (RKI) BAY 43-9006. Int J Clin Pharmacol Ther 2003;41:616–7.
27. Gupta AK, Cerniglia GJ, Mick R, et al. Radiation sensitization of human cancer cells *in vivo* by inhibiting the activity of PI3K using LY294002. Int J Radiat Oncol Biol Phys 2003;56:846–53.
28. Wachsberger P, Burd R, Dicker AP. Tumor response to ionizing radiation combined with antiangiogenesis or vascular targeting agents: exploring mechanisms of interaction. Clin Cancer Res 2003;9:1957–71.
29. Lee CG, Heijn M, di Tomaso E, et al. Anti-vascular endothelial growth factor treatment augments tumor radiation response under normoxic or hypoxic conditions. Cancer Res 2000;60:5565–70.